1A4-2

Non-Foster Enhancements of Electrically Small Antennas

#Richard W. Ziolkowski[1], Ning Zhu[1], Ming-Chun Tang[1,2]

[1] Department of Electrical and Computer Engineering, University of Arizona
1230 E. Speedway Blvd., Tucson, AZ 85721-0104, USA
ziolkowski@ece.arizona.edu, nzhu@email.arizona.edu
[2] Institute of Applied Physics, University of Electronic Science and Technology of China
Chengdu, 610054, People's Republic of China

1. Introduction

Various attributes of metamaterials have led to their consideration for engineering metamaterial-inspired structures for a variety of applications. This includes the miniaturization of resonators and their use for improving the performance characteristics of electrically small antennas from the microwave region up through to the optical region. Achieving higher directivity from electrically small antennas by introducing structured ground planes has been considered successfully. Active metamaterial constructs have been introduced to increase the bandwidths at low frequencies and to overcome the losses at high frequencies. They have led to recent non-Foster antenna designs and experiments. Thus the development of an efficient, high directivity, large bandwidth electrically small antenna is rapidly becoming a possibility.

Electrically small antennas have gained much attention and have been extensively studied, especially in the last decade, for a variety of wireless applications because of their compact dimension advantages in terms of the operational wavelength. A number of efficient metamaterial-inspired designs have been obtained and validated experimentally [1]. However, because of their small electrical sizes, their directivities are near to those obtained from similar sized electric or magnetic dipoles and their bandwidths are extremely narrow. Consequently, it is of great practical interest for a variety of applications to design an efficient electrically small antenna (EESA) with interesting directivity properties, e.g., large front-to-back ratios and gains exceeding those of a patch antenna. Similarly, the bandwidths of passive electrically small antennas are constrained by physical limitations. Consequently, it is also of great practical interest to consider active approaches to achieve large frequency bandwidths.

2. Highly Directive EESAs

One of the approaches to enhance the directivity of antennas has been to integrate known resonant antennas with electromagnetic band-gap (EBG) structures and other types of structured ground planes. Examples include: a CPW-fed cavity-backed slot antenna (EBG consisting of an array of rectangular patches, back plate mounted for additional directivity, 10.3 dB measured gain, 25 dB front-to-back ratio, 85% overall efficiency with ka = 6.66 at 2.45 GHz) [2]; a microstrip patch antenna (spiral-like unit cell EBG, 5.8 dB measured directivity, ~12 dB front-to-back ratio, 95% measured overall efficiency at 2.4 GHz with ka = 3.20) [3], and a metamaterial-inspired electrically small antenna (degenerate band edge-based ground plane, 6.9 dB broadside gain, 95% overall efficiency at 2.59 GHz with ka = 1.95) [4]. While the performance characteristics of all these antennas are admirable, their structured ground planes are non-trivial and not electrically small. We have considered [5] a simpler structured ground-plane approach, i.e., a slotted, finite, parasitic ground plane, to achieve similar efficiencies, enhanced directivities and front-to-back ratios in an electrically small antenna.

We selected the electrically small Egyptian axe dipole (EAD) antenna as the element to be integrated with the structured parasitic ground plane. As with other metamaterial-inspired near-field resonant parasitic (NFRP) EESAs [1], the EAD EESA is nearly completely matched to a 50 Ω

source (by choice) with no matching element and exhibits a high overall efficiency. However, because it is electrically small, it simply exhibits the directivity associated with a small dipole antenna (~ 1.5 or 1.76 dB). While its integration [6] with a magnetic dipole increased its front-to-back ratio (from 0 dB to 17.1 dB) and its directivity (4.5 dB) to near the theoretical maximum (2 × 1.5 = 3.0 or 4.77 dB), even a higher directivity and a larger front-to-back ratio would be desirable for many wireless applications. We have found that integrating the EAD EESA with a small parasitic ground plane with "two dragons playing pearl" shaped slots, as shown in Fig. 1, leads to an entire system that is low profile and has an electrically small size with $ka = 0.94 < 1.0$; has increased the directivity from 1.77dB to 6.32dB (a 4.55dB improvement); has increased the front-to-back ratio from 0 dB to 23.16 dB; has a half-power beam-width that is large; and has a radiation efficiency of 86.87 % with nearly complete matching directly to a 50 Ω source. Comparing this proposed system to existing approaches, such as a conventional coax-fed circular patch antenna, our proposed antenna system has several advantages. Given the simplicity of its design, which would lead to a low-cost fabrication, its compact size, and its superior performance characteristics, the proposed antenna may be attractive for a variety of wireless systems applications. We have also considered the directivity of a two element array based on this antenna [7]. A broadside directivity of nearly 10dB can be achieved.

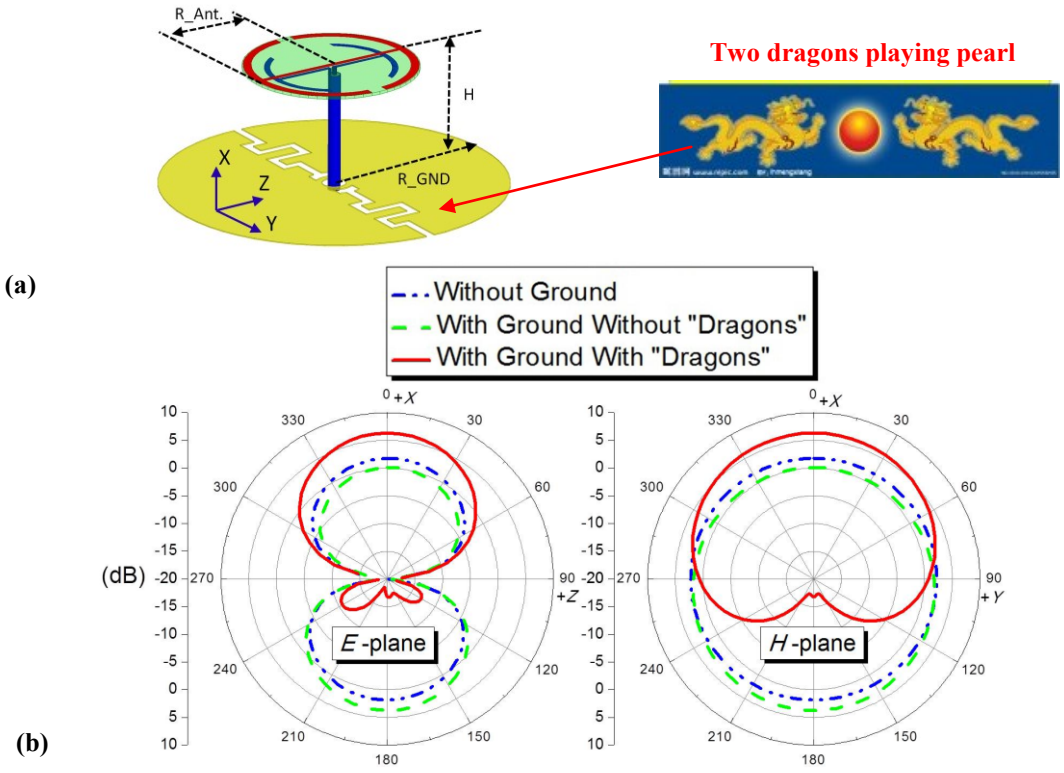

Fig. 1 The Egyptian axe dipole (EAD) antenna integrated with the meandered-slot modified, finite ground plane. (a) 3-D view with design parameters and "two dragon playing pearl" logo, and (b) comparisons of the directivity patterns in *E*- and *H*-planes when $H = 100$ mm, $R\_GND = 150$ mm ($ka_{System} = 0.94$), $R\_Ant = 75.8$ mm ($ka_{EAD} = 0.48$) at 300 MHz for the EAD alone, for it being integrated with the finite ground plane, and for the entire system. [5]

3. Non-Foster Broad-bandwidth EESAs

Because of their small dimensions, EESAs are narrow-bandwidth devices, their bandwidths being restricted by the rather stringent Chu-Thal physical bounds. However, by introducing active elements, these passive bounds are no longer relevant and large bandwidths can be achieved in principle. In particular, by augmenting their narrow bandwidth counter-parts with internal non-Foster elements, active metamaterial unit cells based on negative impedance convertor (NIC) circuits have been introduced as NFRP elements [8, 9]. We have characterized numerically several realistic designs of broad bandwidth metamaterial-inspired NIC-augmented electric and magnetic antennas [8, 9]. The driven and NFRP elements in each presented case are designed to achieve nearly complete matching of the entire system to a 50 Ω source without any matching network and to yield high radiation efficiencies over their FBW_{10dB} bandwidths that are orders of magnitude larger than their passive counterparts. A 300MHz version of the planar protractor NFRP antenna was designed, as shown in Fig.2a, for fabrication with Rogers 5880 Duroid™. The NFRP element (red object on the front side) is driven by the coax-fed monopole (yellow object on the back side). The HFSS-simulated $|S_{11}|$ values are shown in Fig. 2b from 200 to 400MHz. This ka = 0.48 protractor antenna achieves a -22.7 dB $|S_{11}|$ value at f_{res} = 300 MHz, and its 10dB bandwidth is 1.6 MHz (from 299.3 MHz to 300.9 MHz). The resonant frequencies for different capacitance values across the gap in the protractor NFRP element, as predicted by HFSS-ADS co-simulations, are also shown in Fig.2b. The resonant frequency could be tuned between 202.8 and 395.9 MHz, with ideal capacitance values changing from 1.5 pF to -0.6 pF, without changing any of the dimensions of the protractor antenna. However, capacitance values which would reproduce a fit to the dashed blue curve, particularly the negative values and those needed to match the large slopes involved, cannot be achieved with purely passive circuit elements. However, with a properly designed NIC-circuit, they can be. The bandwidth results for the NIC-augmented protractor NFRP antenna are shown in Fig. 2c. They yield a 147.5 MHz 10dB bandwidth, *a 92-times increase*, with large overall efficiencies over this band. We have confirmed the stability of the NIC circuits for both antennas using time domain simulations. We have preliminary experimental results that demonstrated almost a factor of 10 increase in the bandwidth [9]. We are currently using another EESA design in experiments to try to verify that these results can be improved even more.

References

[1] R. W. Ziolkowski, P. Jin and C.-C. Lin, "Metamaterial-inspired engineering of antennas," Proc. IEEE, vol. 99, pp. 1720-1731, Oct. 2011.

[2] J. Joubert, J. C. Vardaxoglou, W. G. Whittow, and J. W. Odendaal, "CPW-fed cavity-backed slot radiator loaded with an AMC reflector," IEEE Trans. Antennas Propag., vol. 60, pp. 735-742, Feb. 2012.

[3] R. Baggen, M. Martínez-Vázquez, J. Leiss, S. Holzwarth, L. S. Drioli and P. de Maagt, "Low profile GALILEO antenna using EBG technology," IEEE Trans. Antennas Propag., vol. 56, pp. 667-674, Mar. 2008.

[4] G. Mumcu, K. Sertel, and J. L. Volakis, "Miniature antenna using printed coupled lines emulating degenerate band edge crystals," IEEE Trans. Antennas Propag., vol. 57, pp. 1618-1624, Jun. 2009.

[5] M.-C. Tang and R. W. Ziolkowski, "Improving the directivity of electrically small antennas using a slot-modified, finite, parasitic ground plane," submitted to IEEE Trans. Antennas Propag., March 2012.

[6] P. Jin and R. W. Ziolkowski, "Metamaterial-inspired, electrically small, Huygens sources," IEEE Antennas Wireless Propag. Lett., vol. 9, pp. 501-505, May 2010.

[7] M.-C. Tang and R. W. Ziolkowski, "A compact, two-element array with ultra-high broadside directivity," submitted to IEEE Trans. Antennas Propag., April 2012.

[8] N. Zhu and R. W. Ziolkowski, "Active metamaterial-inspired broad bandwidth, efficient, electrically small antennas," IEEE Antennas Wireless Propag. Lett., vol. 10, pp. 1582-1585, 2011.
[9] R. W. Ziolkowski and N. Zhu, "Non-Foster element, bandwidth enhanced, metamaterial-inspired electrically small antennas," International Workshop on Antenna Technology, iWAT 2012, paper 7.4, Tucson, AZ, Mar. 2012.

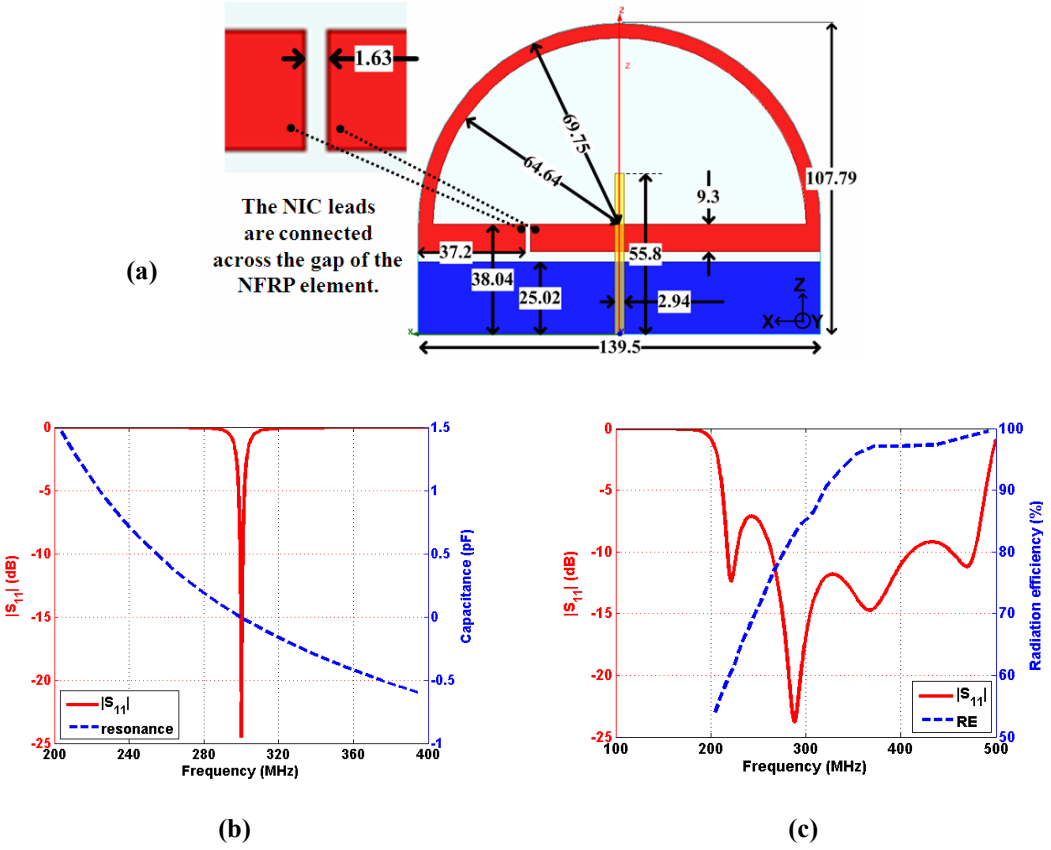

Figure 2. (a) The 50 Ω, 300 MHz, protractor antenna, all dimensions are in mm. (b) Its simulated performance characteristics. $|S_{11}|$ values (red) and curve fitting results of the capacitance values required to achieve the resonant frequencies in this band (blue). (c) The corresponding NIC-augmented protractor antenna results. The $|S_{11}|$ values show a much broadened bandwidth (red) and the curve fitted results of the radiation efficiency (blue) exhibit high values across the -10dB operational bandwidth.